4-25-2023

Base Vibration Effects on Additive Manufactured Part Quality

N. J. Jensen
Tokyo Institute of Technology

G. G. Parker
Michigan Technological University, ggparker@mtu.edu

J. R. Blough
Michigan Technological University, jrblough@mtu.edu

Follow this and additional works at: https://digitalcommons.mtu.edu/michigantech-p

Part of the Mechanical Engineering Commons

Experimental Techniques
https://doi.org/10.1007/s40799-023-00629-1

APPLICATIONS PAPER

Base Vibration Effects on Additive Manufactured Part Quality

N. J. Jensen[1] · G. G. Parker[2] · J. R. Blough[2]

Received: 16 June 2022 / Accepted: 9 January 2023

Abstract

Additive Manufacturing (AM) has opened the door for portable and self-sufficient fabrication. However, environments with base vibration degrade part quality during production. This work focuses on investigating and mitigating the effects of base vibration on AM part quality. Factors influencing part quality initiated the approach, followed by experiments on an extrusion-type printer to inspect and minimize vibration effects. Part roughness was used as the part quality metric based on preliminary experimental observations. A modal impact test identified the print bed and print head gantry as vibration-sensitive components at $\approx$ 40 Hz. These vibration modes were targeted with experiments to evaluate and reduce vibration effects. Vibration originating from machine operation and vertical base vibration were compared. Part quality was impacted by base vibration 600$\times$ more than by machine operation. Part roughness correlated with vertical base vibration intensity as the roughness standard deviation increased over 85%, from 187.71 μin to 349.01 μin, for parts printed with base vibration compared to parts printed without. This result indicated base vibration as the primary vibration source that leads to part quality degradation. A passive vibration control scheme was implemented resulting in a 93% reduction in the relative motion between the print head and bed, from 23.71 to 1.75 g/g, and a 16% improvement in part surface roughness, from 1015.60 to 850.39 μin. This research provides direction for extending AM to harsh operational environments.

Keywords Base vibration · Extrusion printing · Modal impact test · Part roughness · Part quality · Vibration control

Introduction

Machine Limitations in Harsh Environments

Additive Manufacturing (AM) has many benefits for permanent and mobile fabrication. Many AM users are attracted to its features including low footprint, weight, and increased agility. The marine industry, for instance, considers using AM for generating parts that can withstand corrosive and dynamic conditions [1]. However, mobility and compactness comes with one side effect that hinders AM's widespread adoption: deficient part quality produced in vibratory environments. The vibratory nature onboard ships due to base vibration disrupts extrusion-based AM processes by exciting a printer's structural vibration modes [2]. The excited modes lead to misaligned machine components that create unlevel part structures [1], resulting in poor print accuracy.

3D printers can be classified as precision machines. Precision machines are machines which performance can be undermined without mitigating vibration [3]. The vibration source affecting precision machines could be from its operation or the structure it rests on. Machine vibration is often a result of rapid moving machine components, while base vibration originates from external factors like nearby vibrating machines. Both of these effects on machine performance have been studied for decades [3, 4]. Although the ideal solution for such devices is to redesign the environment to minimize environmental vibration [5], it is typically high-cost and excessive for most scenarios. Therefore, efforts to mitigate environmental vibration

✉ N. J. Jensen
jensen@lim.sc.e.titech.ac.jp

G. G. Parker
ggparker@mtu.edu

J. R. Blough
jrblough@mtu.edu

1 Department of Systems and Control Engineering, Tokyo Institute of Technology, Ookayama, Meguro, Tokyo, 152-8552, Japan

2 Department of Mechanical Engineering—Engineering Mechanics, Michigan Technological University, Houghton, MI 49931, USA

Published online: 25 April 2023

affecting precision machine performance pursue two common strategies: 1) adaptive machine control that compensates for the machine or base vibration and 2) active or passive isolation.

The first approach was carried out by Duan et al., where they used a feedforward control algorithm, informed by the printer's near-future route, to minimize an extrusion printer's trajectory during production [6]. Rivin engaged the second method by passive and active isolation and suggested that passive isolation is sufficient for most scenarios [7]. Rivin found that active isolation is beneficial when a process requires extreme machine precision [7]. Though isolation has primarily been pursued as a mitigation strategy to *decouple* the equipment's vibration source from the structural vibration modes, recent work has shown how designed *coupling* of the isolation devices with the machine's structural vibration modes can reduce unwanted vibration for horizontal and rocking motion [8].

State of Research

Regardless of the scheme to mitigate vibration affecting a precision machine, understanding a machine's vibration response is vital [5, 9]. To the authors' knowledge there exists few studies about vibration affecting extrusion-type 3D printers. Two groups investigated how fast repositioning of AM print heads excited the printer's structural vibration modes and affected part surface roughness [10, 11]. Neither references explored base vibration effects and how it contributes to AM part quality. This paper extends the current research by answering two questions: 1) *what is the affect of base vibration on AM part quality?* and 2) *how can part quality degradation be mitigated?*

Research Approach

In light of the research questions stated above, this paper has four contributions based on experiments with an extrusion-type printer:

1. Vertical base vibration dominates a printer's vibration response, not machine vibration.
2. Relative vertical motion between a printer's bed and gantry degrade part quality.
3. Part quality deteriorates with increased base vibration, both qualitatively and quantitatively as measured by surface roughness.
4. Passive isolation can improve part quality in the presence of base vibration.

The first contribution was determined by two tests during AM parts production: one excited the printer's vibration modes with machine vibration and vertical base vibration; the other excited the printer's vibration modes with machine vibration only. The printer's bed and head relative vertical motion data was used to determine which vibration source dominated the printer's response (ref. "The Source and Effects of Part Quality Degradation" section). The second contribution pursued a modal impact test to identify vibration-sensitive printer components. High-energy vibration modes appeared on the print bed and print head gantry at $\approx$ 40 Hz. These components were then targeted to quantify the correlation between vertical base vibration and part quality (ref. Sections 2 and 2). The third contribution was based on considering the print bed and print head relative vertical motion during part production versus part surface roughness when exposed to vertical base vibration. The printer's bed and head relative motion data was recorded while the printer discharged a layer of material. Data were extracted from the relative motion record to inspect the printer's average vertical movement irrespective of its configuration. Part roughness was observed and measured to assess part quality (ref. "The Source and Effects of Part Quality Degradation" section). The final contribution involved implementing a passive isolation scheme to mitigate the base vibration effects on AM part quality (ref. "Passive Base Isolation" section).

The remainder of this paper describes the approach for measuring AM part quality, the process of identifying vibration-sensitive printer components, the experiments to identify the source of vibration that leads to part quality degradation, and implementing a passive vibration control solution to demonstrate improved AM part quality. The overall approach is highlighted in Fig. 1 showing some general [12] and research specific factors that influenced the part quality metric decision. The paper concludes by discussing the experimental results and the implications for other AM equipment that could be placed in vibratory settings.

Additive Manufactured (AM) Part Quality

This section focuses on the factors that led to using surface roughness as the part quality metric. First, some general factors from the literature are discussed followed by preliminary vibration test results. Several parts were printed on an AM printer while it was excited by vertical base vibration to measure the effects on part quality. The observed effects contributed to the final part quality metric decision of averaged surface roughness (Ra). This section closes with a brief discussion of how surface roughness measures direct effects of parts printed amidst vibration and how it indicates indirect part effects like dimensional inaccuracies and wear intolerances.

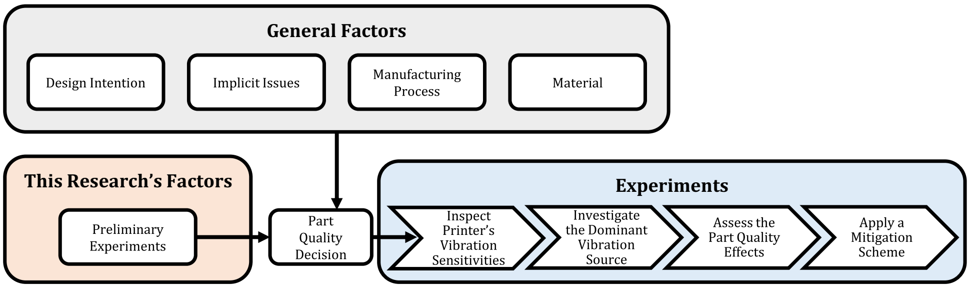

Fig. 1 Overall approach for this research to explore vibration effects on 3D printing. The general and research specific factors were considered for the part quality metric decision. The general factors are common in the AM literature [12]. The research's factors are additional for the research at hand where preliminary experiments indicated vibration effects on part quality. Following the part quality metric decision, a series of experiments were performed to identify the vibration effects on the quality metric and mitigate effects that degrade part quality

Factors and Measures

The quality of AM parts may be subjective. General factors in Fig. 1 are a few that influence how part quality is assessed; they include design intention, implicit issues, manufacturing process, and material [12]. Design intention is often the focus for assessing part quality. Any of the following may be important for a given design: strength, durability, density, number and type of allowable defects, and dimensional accuracy. One widespread design concern is part strength [13], which can be used for understanding if, how, and when a part may fail in its prescribed environment. On a different note, identifying and minimizing part defects [14, 15] has also been essential for AM processes as they focus on reproducible production.

Implicit part quality issues, issues that are an indirect result of another, can influence how one chooses a part quality metric. Surface quality is one instance where a part's surface can be measured directly and indicate implicit part quality features like geometric inaccuracy and part misfunction [12]. AM processes, on the other hand, have specific traits that influence a final part and its quality. The AM printer used in this research is a FDM type that uses extrusion to print. Compared to another process like powder bed fusion (PBF), PBF is more prone to part vacancies so this would factor differently for a part quality decision. Material choice also shares in how part quality is evaluated. Plastics, metals, ceramics, and composite AM materials have varying mechanical and physical properties resulting in different perspectives when analyzing the part quality of each. Together these factors influence decisions for measuring part quality in a given situation. Regardless of a study's breadth to establish a catch-all part metric, the situation still resolves to subjectivity, as indicated by Udroiu et al. [12].

For this study, an additional factor from Fig. 1 was considered before selecting part surface roughness as the part quality metric: preliminary experimental observations. Preliminary experiments vibrated the printer and informed the decision by indicating surface quality effects, which is discussed in the next section.

Part Roughness

This research focused on extrusion-based PETG parts (material sourced from [16]). The chosen quality metric was average surface roughness (1). Equation 1 comprises measured distances of orthogonal points $|z(x)|$ along a surface profile x. The points are averaged for the surface length l to give a surface roughness value R_a.

$$R_a = \frac{1}{l}\int_0^l |z(x)|dx \tag{1}$$

The metric was chosen for four reasons:

1. It numerically characterized one of the effects observed during preliminary vibration testing.
2. Measurements correlated to visual assessment.
3. Measurements are repeatable using a profilometer.
4. Correlates to implicit issues like geometric inaccuracies.

Preliminary Experimental Observations

Figure 2(a) illustrates surface roughness effects from base vibration by contrasting parts made with and without vertical base vibration. The front-view of two PETG AM extruded parts are shown in this figure. The top part was generated without vertical base vibration, and the bottom part was produced with it. The highlighted regions on each illustrate the detrimental effects on the part surface that were observed and used to guide the part quality metric selection. Observed layer degradation indicates part quality issues like surface roughness explicitly and dimensional inaccuracies implicitly. The geometry of each part is displayed in Fig. 2(b) with locations highlighted to show where roughness measurements were acquired. The part's base is approximately 2"x2". The numbered

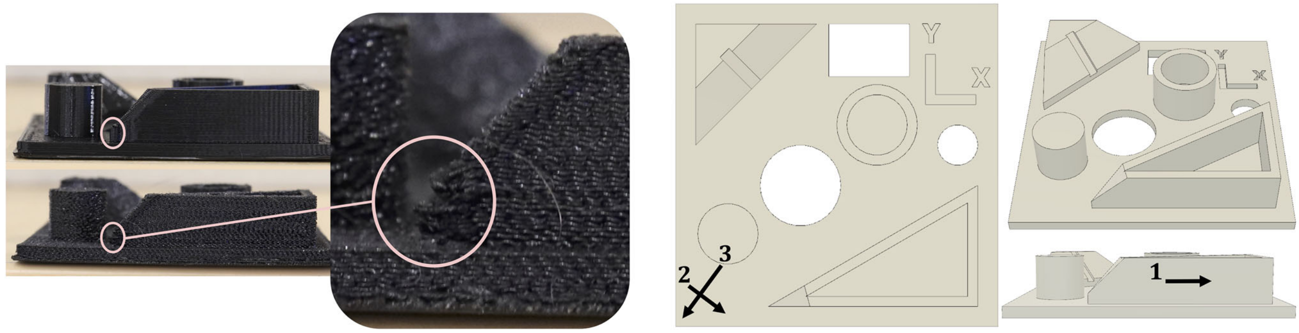

(a) Front-view of two PETG AM parts produced by an extrusion process. The top part was generated without vertical base vibration, and the bottom part was produced with it. The highlighted regions on each illustrate the detrimental effects on the part surface that were observed and used to guide the part quality metric selection.

(b) Part geometry and roughness measurement locations. Location 1 shows the place and direction for measurements on the feature face, location 2 shows another spot on the bottom left corner of the part's top-view, and location 3 represents the same spot as location 2 but in a perpendicular direction.

Fig. 2 Preliminary surface roughness observations and measurement diagram

locations indicate the direction of surface roughness measurements that were acquired using a Mitutoyo SJ-210 profilometer (see "Forced Vibration Tests" section for instrument details). Location 1 shows the place and direction for measurements on the feature face (with the printing grain/direction), location 2 shows another spot on the bottom left corner of the part's top-view (with the printing grain/direction), and location 3 represents the same spot as location 2 but in a perpendicular direction (against the printing grain/direction). Part roughness measurements were acquired at several locations to understand how different surface directions were affected by vibration. Table 1 provides a list of the roughness values recorded for each part shown in Fig. 2(a) and indicates that the same pattern of the vibrated part being rougher exists in each measurement location and direction. This common result led to focusing on only on measurements at location 3 to simplify the discussion for the remainder of this research.

Annotating both parts in Fig. 2(a) are circles that emphasize the effects of vertical base vibration. One noticeable difference between these two is the layer degradation at the edge of the indicated feature. The highlighted region has a straight edge in the photo where no vibration was present, whereas the part printed with vibration fails to keep the feature straight. These observations provided sufficient evidence for confidence in selecting surface roughness to gauge part quality.

Implicit Issues

Although the results discussed above were the primary reasons for selecting part roughness as a measure of AM part quality, this metric likely correlates with other part deficiencies. Assembly variation, dimensional inaccuracies, and wear intolerances are a few that have been explored – primarily for AM with metal materials – in the literature [12, 17, 18]. Although the literature's material and processes are different from what is considered here, the results informed this work. For instance, it was recently demonstrated that surface roughness was directly related to the fatigue life of powder bed fusion produced metal parts, meaning a rougher surface leads to a shorter fatigue life [18]. This agreement further supports the choice to use roughness to assess part quality.

Experiments

This section describes the experimental approach shown in Fig. 3. A modal impact test was performed to identify vibration-sensitive printer components before pursuing the vibration effects experiments. A single frequency of vertical base vibration was applied to the printer rigidly mounted to an ES-10D-240 Dongling shake table. Two sets of parts were printed, and their surface roughnesses were assessed:

Table 1 Part roughness values of two parts shown in Fig. 2(a) for the locations in Fig. 2(b). Bolded is the roughness measurement that was used for the remainder of this research

Measurement	Ra Roughness (μin) No Vibration	Ra Roughness (μin) With Vibration
1	77.24	1256.00
2	143.82	951.40
3	**237.65**	**946.15**

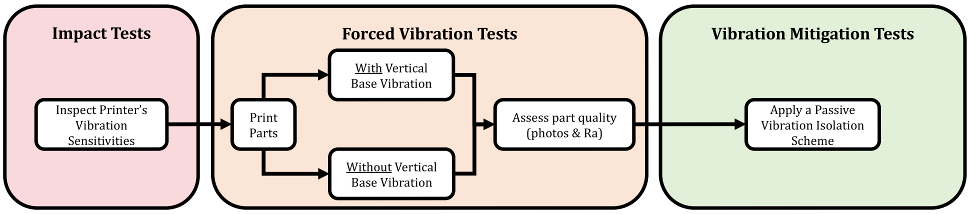

Fig. 3 A modal impact test proceeded the vibration effects experiments identifying vibration-sensitive components to target with vertical base vibration. A passive vibration control scheme was implemented to demonstrate a solution to mitigate vibration effects on part quality

one set with and one set without vertical base vibration. Subsequent vibration effects experiments were designed to investigate how base vibration excites a printer's structural modes and its effects on AM part quality. A passive isolation scheme was then implemented to mitigate base vibration effects on AM part quality. The subsections below describe the experiments in detail.

Impact Tests to Identify Vibration Sensitive Components

The forced vibration tests were preceded by impact tests to identify vibration-sensitive printer components shown in Fig. 4. The printer model was a MakerBot Method X printer, with a dimensional accuracy of 0.2 mm. Its composite housing was supported with steel and aluminum substructures. A load-cell instrumented hammer was used to strike the printer in various locations while accelerometers measured its response.

Sensor locations were explored to identify printer components that directly affected print quality. The print bed and print head gantry were candidates as their motion has a primary role in printing a part's geometry. Other areas were excluded based on testing the vibration response at specific points because they had measurable compliance. Compliance does not lend to clear results through modal analysis, so these areas were not considered further. A few examples were the gantry's corner drive mounts, the X-Z face of the gantry and print heads, and the Y-Z face of the print heads.

Once sensor locations were established, two testing scenarios in Fig. 4 were set up: one with impacts and measurements on the print bed (left photo), the other setup with the print head gantry (right photo). This process was repeated for several impact locations and used to compute modal frequencies and mode shapes. Since modal analysis relies on a static configuration of a structure, several configurations were tested to understand how the printer's vibration modes varied with the print head and print bed positions. The varying configuration tests were not exhaustive though they showed that print bed mode frequencies and shapes *did not* vary with the print bed or print head positions, and gantry modes *did not* vary with print bed position, though they varied with print head position.

Two example frequency response functions (FRFs) from the tests are shown in Fig. 5. FRFs in the top left and top right, coherence (left bottom), and phase (right bottom) for the print bed and print head gantry as indicated in Fig. 4. Three vibration modes are present: one on the print head gantry at $\approx$ 38 Hz, on the print bed at $\approx$ 47 Hz, and at $\approx$ 58 Hz on the print head gantry. The shaded region centers

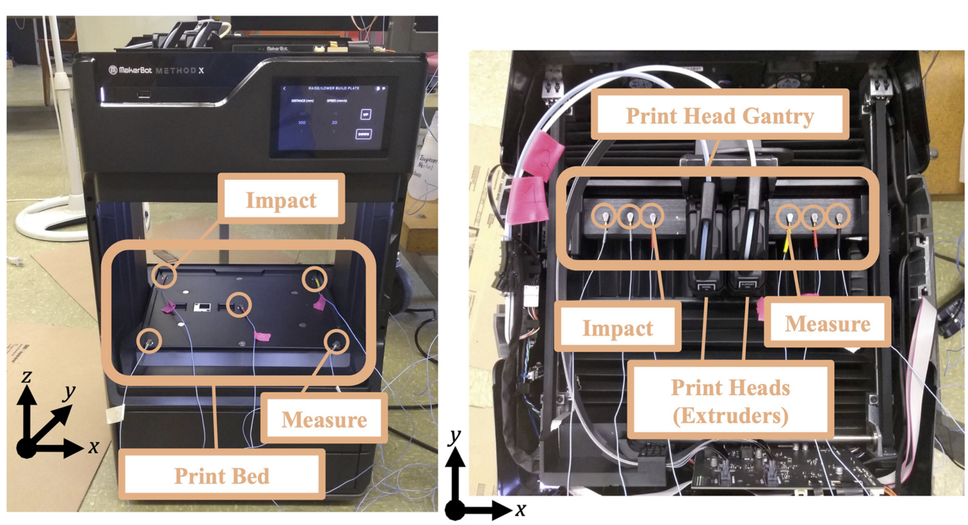

Fig. 4 Experimental setup for the modal impact test that preceded the vibration effects experiments. Accelerometer locations are circled on the print bed and print head gantry. Impact and measurement locations are indicated for results discussed in Fig. 5

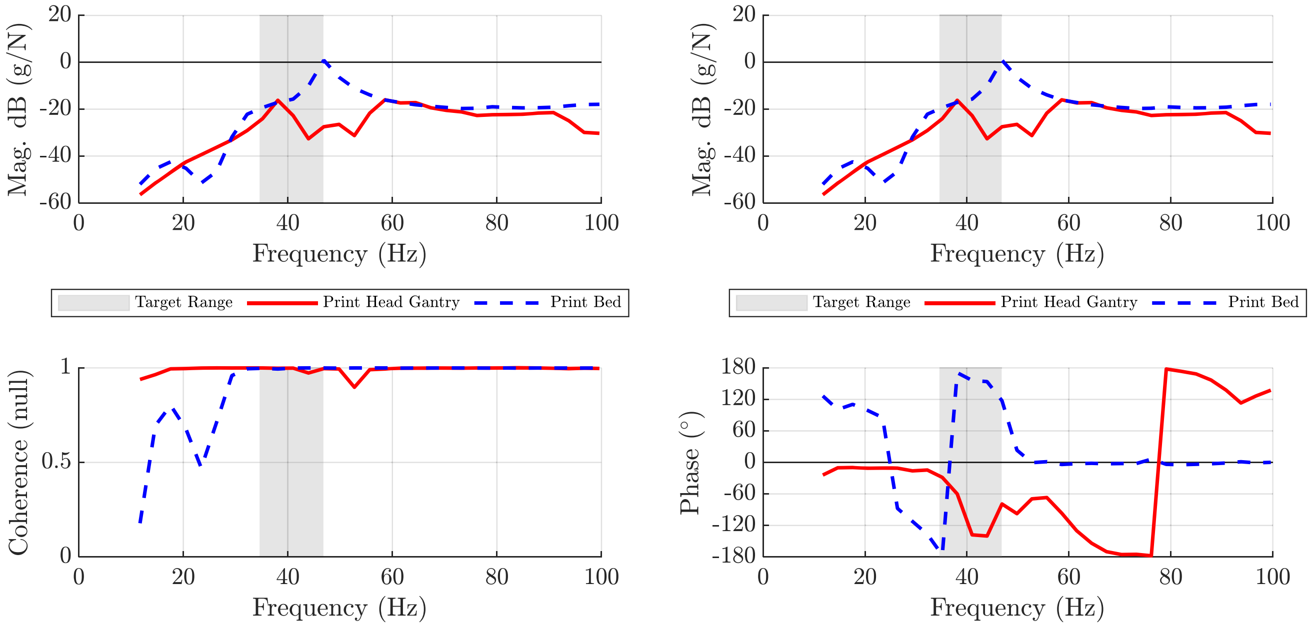

Fig. 5 Frequency response function estimates (FRFs) in the top left and top right, coherence (left bottom), and phase (right bottom) for the print bed and print head gantry as indicated in Fig. 4. The shaded region centers on 40.7 Hz with a 10% bound in either direction, which was the frequency range for the vibration effects experiments' excitation

on 40.7 Hz with a 10% bound in both directions, indicating the excitation range for subsequent forced vibration tests described in "Forced Vibration Tests" section. The impact test observations are summarized as:

1. A high-energy vibration mode manifested at $\approx$ 40 Hz on the print bed and print head gantry.
2. The print bed corners and midpoint had the largest motion.
3. The resonant motion of the print bed and print head gantry occurred within a small frequency range, which indicated a possible large relative motion between them.

Forced Vibration Tests

Forced vibration tests were used to determine the effect of base excitation on part quality. The approach measured relative acceleration between the print head and bed while printing and related it to part quality. The experimental setup is described below and shown in Fig. 6.

The printer was mounted to the Dongling shaker using Vibration Research VibrationVIEW (ver 10) to control the shaker. Two custom mounting plates – spaced with aluminum inserts – connected the printer's base and the shake table's head expander. Two PCB® accelerometers recorded vibration intensity, a 352A24 under the print bed center (origin of the parts built) and a 352C22 on the top of the primary print head. Each channel recorded data while the stepper motor belt driven gantry (with X-Y motion) and stepper motor leadscrew driven print bed (with Z motion) moved during part production shown in Fig. 7. A Simcenter SCADAS XS data acquisition (DAQ) system configured with Simcenter Testlab 2019.1 recorded the measurements. Vibration came from two sources: the machine's vibration and the vertical shaker. The machine's vibration was excited by rapid print head motion with the printer set to a max print head travel speed of 500 $\frac{mm}{s}$. Vertical excitation amplitude ranged between 0.0325 and 0.13 g. A series of tests were performed between these amplitudes. The input levels were chosen based on the values being below the threshold of where the printer would be damaged by resonance yet high enough to excite the printer. Discrete amplitude setpoints were used with a frequency of 40.7 Hz for the entire print-time. Data collection occurred with a sampling frequency of 2,560 Hz.

Two sets of parts shown in Fig. 2(b) were printed, 10 with vibration and 33 without vibration. The part design included many primitive features like cylinders, cutouts, chamfers, and varying angle edges to represent typical AM features. Although these features could be assessed in various ways, surface roughness was used as described in "Part Roughness" section.

Since the analysis described later in "Results and Discussion" section is based on relative comparisons between parts printed with the same 3D printing parameters (i.e., nozzle temperature, filament feed rate, etc.), the parameters

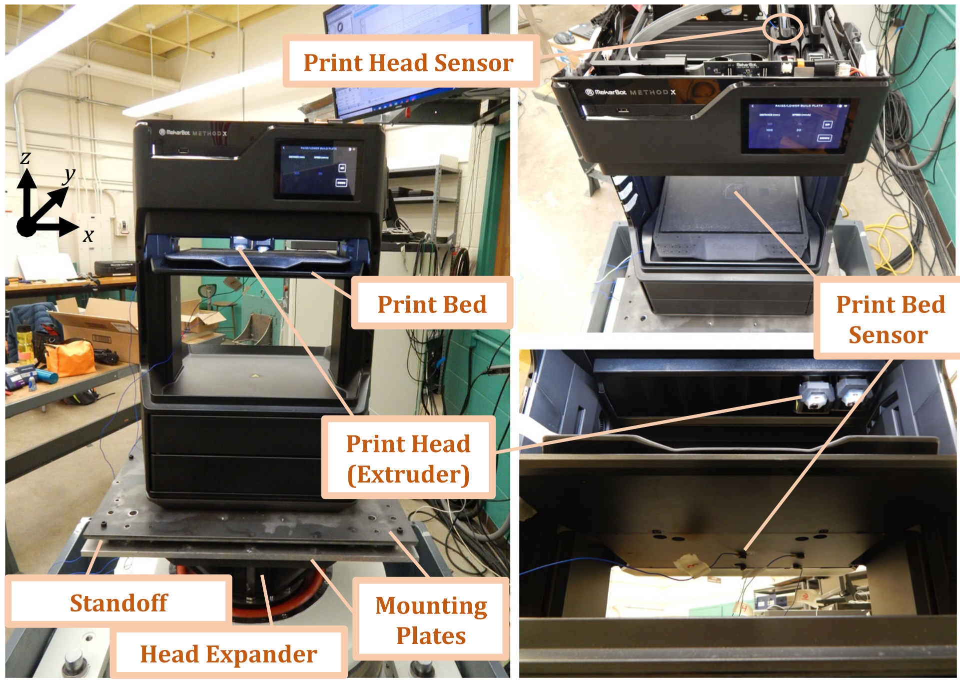

Fig. 6 Experimental setup of the MakerBot Method X printer rigidly mounted to an ES-10D-240 Dongling shaker. Two accelerometers were positioned to measure the vibration of the printer: on top of the primary print head and underneath the center of the print bed where a part would be built

are not provided here. A Mitutoyo SJ-210, featuring a range of 14,200 μin and an error of 0.8 μin was used to measure part roughness as described above. The dissimilar sample sizes of printed parts resulted from needing an observer present for the entire $\approx$ 1 hr production during the vibration tests, but not for tests without vibration.

Results and Discussion

This section contains the key observations from the forced vibration tests. Two subsections identify base vibration as the most significant source of degraded part quality and how these effects can be mitigated to improve part quality.

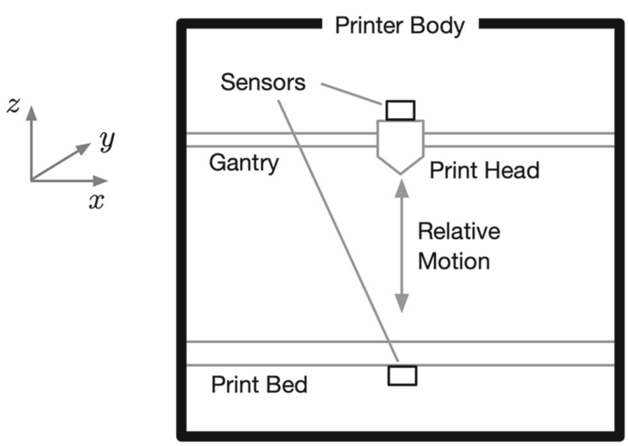

Fig. 7 Test setup illustration to measure bed-head relative motion while printing

The Source and Effects of Part Quality Degradation

Considering the goal of the vibration tests was to capture the effect of base vibration on part quality, it is appropriate to identify the dominant vibration source during production. Figure 8 represents the printer's response to base vibration and machine vibration to illustrate this point.

Before addressing the results, an explanation is needed to clarify where these results originated. The results in Fig. 8 were acquired during a test with the shaker set to a 0.1 g vertical sinusoid at 40.7 Hz for the entire production.

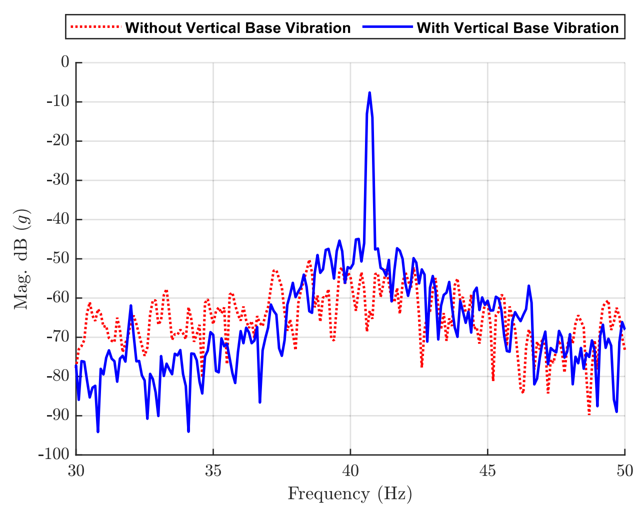

Fig. 8 Relative motion measured between the print head and bed accelerometers (see Figs. 6 and 7)

Sensors in Fig. 7 acquired time-domain data during one production layer. The relative motion of the printer's bed and head shown in Fig. 7 was computed by subtracting the accelerometers' time-histories. These three signals had a 60 second time history that was split from end-to-end into 6 sets of data. A hanning window was applied and the spectral response was computed using the fast-Fourier transform (FFT) with a 0.1 Hz frequency resolution. All datasets were averaged with linear weighting according to (2) to reduce uncorrelated measurement noise, where M is the number of datasets and m is the index for each frequency bin.

$$\bar{x} = \frac{1}{M}\sum_{m=1}^{M} x_m \tag{2}$$

This approach focused on the average acceleration during a printed layer rather than peak responses at different print head positions. And, it was expected for both curves to have a peak at the $\approx$ 40 Hz resonance (see "Impact Tests to Identify Vibration Sensitive Components" section); however, the response with base vibration was larger. For both curves in Fig. 8 machine vibration was present as the print head travel speed was set to a maximum of 500 $\frac{mm}{s}$ to excite the printer's modes. However, Fig. 8 indicates that machine vibration is 600× less significant of a vertical vibration source than base vibration. This was expected since the machine vibration relies on horizontal to vertical coupling to excite the same resonance. More things that could have attributed to the curves' differences are the print heads mass and the printer structure's stiffness and damping in the vertical and horizontal planes. The print heads account for around 2% of the printer total mass. Therefore, only a low amplitude force is exerted for machine vibration. The printer structure also contributed to base vibration being more dominant because of the manufacturer's design intention to stiffen the structure vertically [19]. This design intent explains how the machine vibration was nearly decoupled from the vertical acceleration response. Extended work on this topic may include further testing of horizontal and vertical resonance effects from machine vibration and vertical and horizontal base vibration. Although this result has a condition that makes the comparison less than ideal, it's consistent with the literature that base vibration often dominates machine vibration for precision machines [3, 7, 9].

Two parts from the printed collection are displayed in Fig. 9. The top are of a part printed without vertical base vibration present. The bottom photos are of a part printed while the Dongling shaker excited with 0.13 g vertically at 40.7 Hz. The dominant difference between these parts is the printed layer degradation, which is clear by the non-uniform edges and surface roughness circled in red dots. Such degradation has direct part quality issues like a higher surface roughness, and indirect issues like edge deformation shown in the second photo from the right on the bottom These results are captured by the surface roughness where the standard deviation of parts with base vibration was 349.01 μin and 187.71 μin without, over an 85% increase.

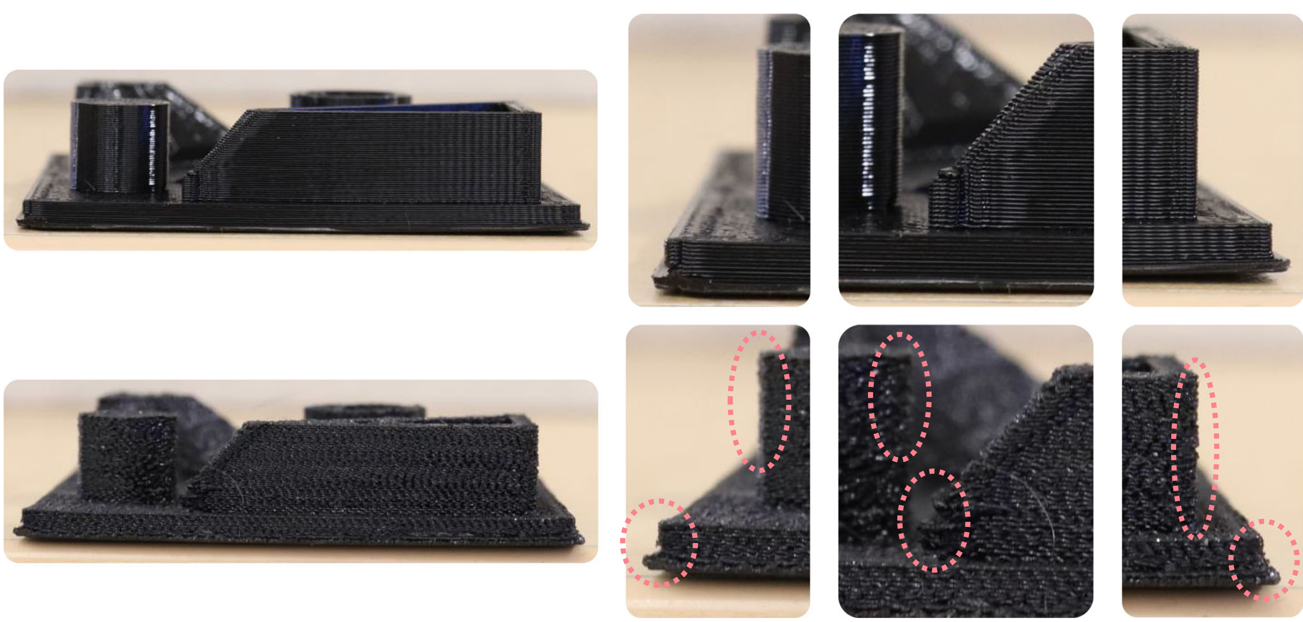

Fig. 9 Photos on the top are of a part printed without vertical base vibration present. The bottom photos are of a part printed while the Dongling shaker excited with 0.13 g vertically at 40.7 Hz

Passive Base Isolation

A passive isolation scheme was implemented to demonstrate vibration mitigation (Fig. 3). Three Inglasco sponge rubber hockey pucks [20] replaced the standoffs shown in Fig. 6 and acted as isolators to decouple the vertical base vibration from the printer's structural vibration. The same experimental setup in Fig. 2 was used to print parts with vertical base vibration, with and without passive isolation. Minimal work was done to tune the passive isolation design, but design work should reduce the vibration and improve the part quality more.

Part photos provided in Fig. 10(a) and 10(b) present the qualitative evidence for improved part quality with reduced vibration. For these images, the focus was on finding a threshold where a part printed with isolation would look similar to one printed without any vibration. For this, a vibration input of 0.0325 g at 40.7 Hz was used for the part shown on the top right and the bottom in Fig. 10(a) and 10(b). The top left photos are from the baseline no vibration case. The part roughness values for these parts corresponded to the visual improvements as the values are shown in Table 2.

Notice ripples in the layers of the part printed with vibration. Compared to the part printed with isolation, the latter has straighter layer edges. For the roughness values, compare the percentage increase from the baseline for with and without isolation. In addition to the parts

Table 2 Part roughness values of two parts shown in Fig. 10 for the regions highlighted in Fig. 2

Part	Ra roughness (μin)	% Above Baseline
Baseline	237.65	–
With Vibration	849.71	257.55
With Vibration & Isolation	290.64	22.30

discussed in "The Source and Effects of Part Quality Degradation" section, part roughness values were recorded for parts produced with passive isolation. These seven samples had an average roughness of 850.39 μin. This result was a 16% reduction compared to those printed without isolation as those ten parts had a mean of 1015.60 μin. This analysis has a weak statistical basis like the discussion from "'The Source and Effects of Part Quality Degradation" section due to its sample size, which could be improved by collecting more samples. Although this passive isolation scheme was not optimized, it improved part quality in terms of qualitative and quantitative part roughness and demonstrated vibration mitigation as a helpful scheme for improving AM part quality.

An alternate perspective in Fig. 11 demonstrates how passive isolation minimized the relative vertical motion of the print bed and print head leading to improved part quality. The data was measured between the print head and print bed accelerometers (see Figs. 6 and 7). The

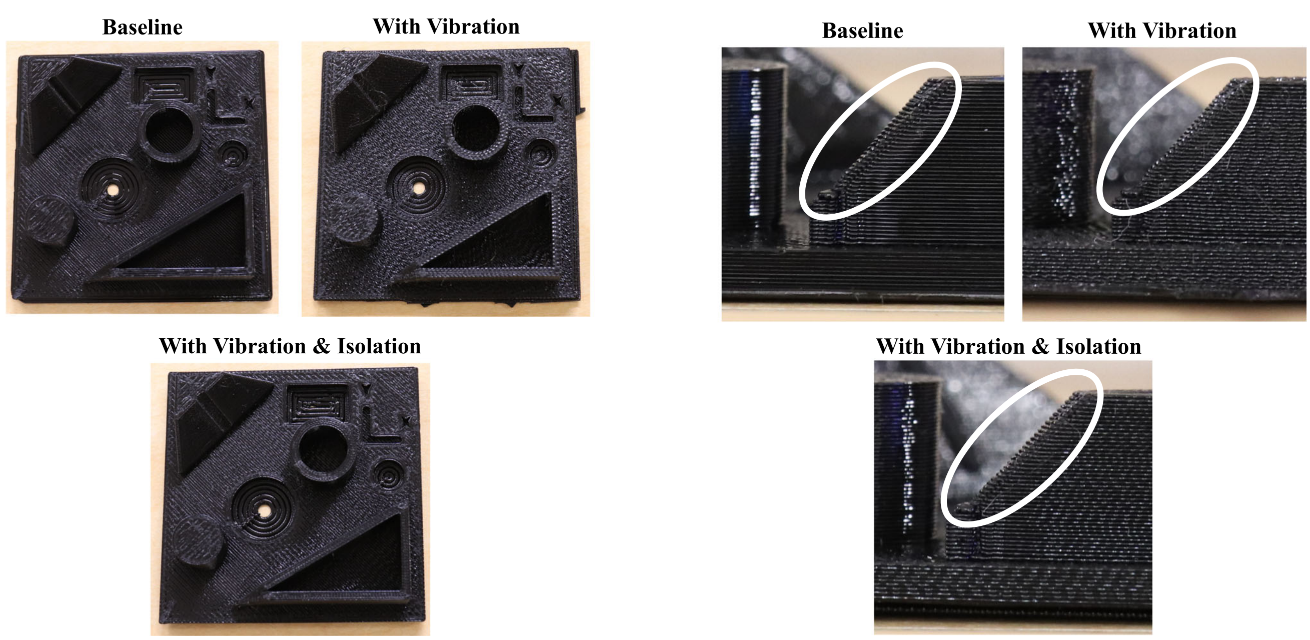

(a) Top-view of parts (b) Front-view of parts

Fig. 10 Photos that show qualitative part quality improvement based on part roughness. Parts were printed with and without vibration at a threshold of 0.0325 g at 40.7 Hz

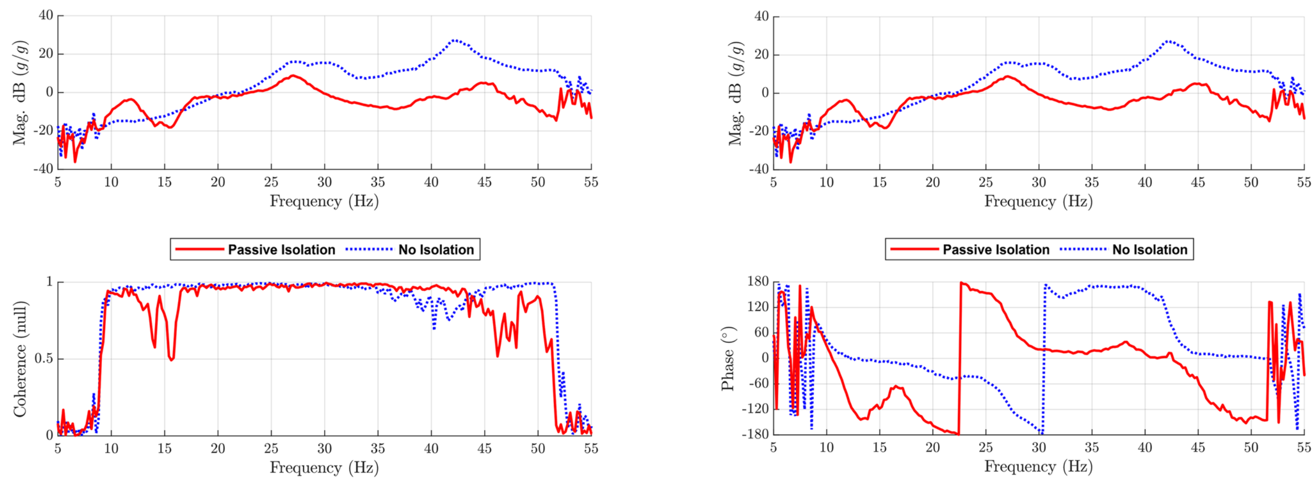

Fig. 11 Relative motion between the print head and print bed for two scenarios: with and without passive vibration control

curves are averaged FRFs computed from accelerometer responses during production. The FRF input was the shaker acceleration and the output was the relative motion. The two curves are from a test without passive isolation and the other with it. The vertical base vibration was set to a random type on the printer at 0.064 gRMS between 10-50 Hz for both cases to target the same resonances described previously. The top plot on the left and right graphics are identical while the bottom plot on the left is the FRFs' coherence and the bottom right is the relative phase between the input and output.

Three frequency regions are annotated in Fig. 11 to show the result of applying passive isolation: at 42, 28, and 12 Hz. At 42 Hz, there is a nearly 93% reduction, from 23.71 to 1.75 g/g, and at 28 Hz there is a 57% reduction in the printer's response, from 6.45 to 2.77 g/g. One side-effect of passive isolation is the higher response at about 12 Hz. In this region, the response with passive isolation is 3.8× larger than without isolation. These results compliment the visual results from Fig. 10 by introducing an alternate perspective of how part quality is affected by base vibration. These FRFs indicate a less time consuming approach to understand how a vibration mitigation strategy may improve AM part quality as this analysis does not require part metrology.

An overall practical approach to understand how base vibration affects AM part quality was given in Fig. 1. However, with the understanding developed through this study, a modified approach is suggested for future work to mitigate vibration effects on AM part quality directly. The adapted approach in Fig. 12 has the same structure as Fig. 1, but with a modified path to go straight from a part quality metric decision to assess how the metric is affected by base vibration and then mitigate it. Although the present work is not exhaustive, this study's results showed that relative vertical motion between the print bed and head dominated the printer's vibration response, which can serve as an assumption for future work. The main thing needed then before analyzing the vibration effects and

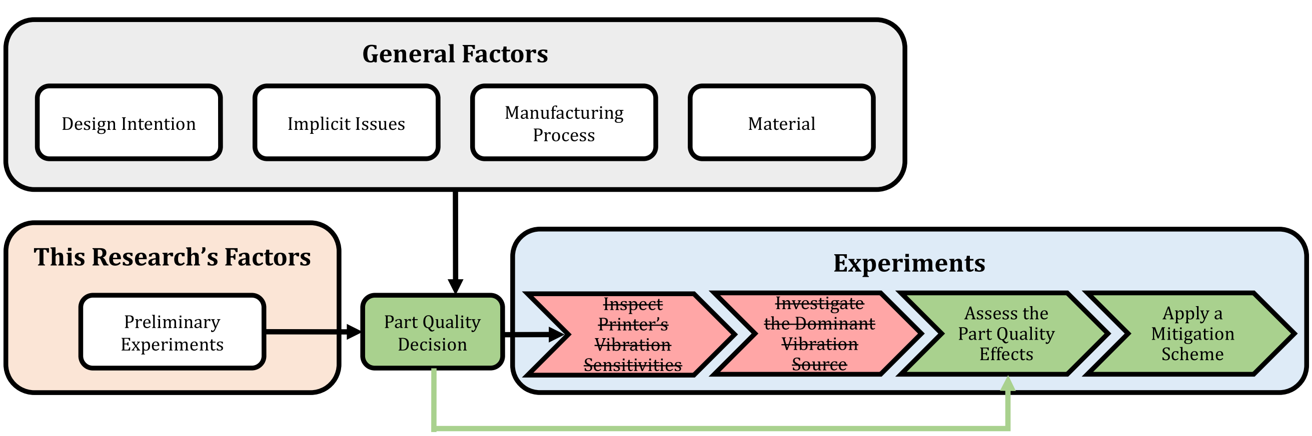

Fig. 12 An adapted overall approach of this research indicates how future work can use the present results to move directly from a part quality metric decision to testing vibration effects and mitigating them. The present results support the assumption that relative vertical print bed and head vibration dominate an extrusion printer's vibration response and should be the focus for applying a vibration mitigation scheme

applying a mitigation strategy is an understanding of the print bed and head relative motion response for a frequency range of interest. Understanding this response would reveal the printer's vibration modes and an allowable amplitude threshold to target with an active or passive vibration mitigation scheme. With the current groundwork laid, the vast literature of vibration mitigation for precision machines can be investigated to select an appropriate scheme to enable AM deployment in harsh environments.

Conclusions

In conclusion, part surface roughness was selected to measure Additive Manufactured (AM) part quality for an extrusion-type printer. The decision was based on common factors from the literature and preliminary experimental observations. The printer's vibration-sensitive components were identified as the print bed and print head gantry in a preliminary experiment. The vibration response of these components were considered to have two sources: machine vibration from rapid printer motion and experimentally induced base vibration. Base vibration effects dominated the response, but future experiments using horizontal excitation and exciting resonances with horizontal components could provide further understanding. The relative motion between these features suggests an area to target with vibration mitigation strategies for similar printers and environments. Part roughness correlated with base vibration intensity for an experiment that vertically vibrated the printer during part production. A passive vibration mitigation scheme was implemented to demonstrate a solution to mitigate vibration effects on part quality. This research illuminates a path for evaluating functionally similar printers before deployment in harsh operational environments. AM is progressing in permanent and mobile fabrication with a few revolutionary areas, including onboard ships, vehicles, or spacecraft. This research reveals how AM can advance beyond static production settings to places it has never been.

Acknowledgements A hearty thanks to Jon Lund and Marty Toth for their help with fixture fabrication, Peter Zach, T.J. Edwards (from ATR Corp.), and MakerBot technical support for their guidance for testing the printer, Cora Taylor for help with the experimental setup, Rachel Store and Nick Hendrickson for metrology support, Jacob Lundin for help with 3D printing, Karavela Zeiter, Julia Barnes, and Artemis Allison for editing assistance.

Author Contributions Nicholas J. Jensen: Conceptualization, Methodology, Formal analysis, Investigation, Writing - Original Draft, Writing - Review & Editing, Visualization. Gordon G. Parker: Conceptualization, Methodology, Formal analysis, Resources, Writing - Review & Editing, Supervision, Project administration, Funding acquisition. Jason R. Blough: Conceptualization, Methodology, Formal analysis, Resources, Writing - Review & Editing, Supervision, Funding acquisition.

Declarations

Competing interests This material is based upon work supported by Naval Sea Systems Command under Contract No. N68335-20-C-0655. Any opinions, findings and conclusions or recommendations expressed in this material are those of the author(s) and do not necessarily reflect the views of Naval Sea Systems Command.

References

1. Strickland JD (2016) Applications of additive manufacturing in the marine industry. In: Proceedings of the 13th international symposium on PRActical design of ships and other floating structures (PRADS' 2016), https://doi.org/10.13140/RG.2.2.29930.31685
2. Jensen N (2021) Base vibration effects on additive manufactured part quality: A study of 3d printing onboard u.s. navy ships. Master's thesis, Michigan Technological University
3. DeBra DB (1992) Vibration isolation of precision machine tools and instruments. CIRP Ann 41(2):711–718. https://doi.org/10.1016/s0007-8506(07)63257-0
4. Perner M, Algermissen S, Keimer R, Monner HP (2016) Avoiding defects in manufacturing processes: A review for automated CFRP production. Robot Comput-Integr Manuf 38:82–92. https://doi.org/10.1016/j.rcim.2015.10.008
5. Gordon CG (1992) Generic criteria for vibration-sensitive equipment. In: Gordon CG (ed) SPIE proceedings, volume 1619. SPIE, https://doi.org/10.1117/12.56826
6. Duan M, Yoon D, Okwudire CE (2018) A limited-preview filtered b-spline approach to tracking control – with application to vibration-induced error compensation of a 3d printer. Mechatronics 56:287–296. https://doi.org/10.1016/j.mechatronics.2017.09.002
7. Rivin EI (1995) Vibration isolation of precision equipment. Precis Eng 17(1):41–56. https://doi.org/10.1016/0141-6359(94)00006-l
8. Lee J, Okwudire CE (2016) Reduction of vibrations of passively-isolated ultra-precision manufacturing machines using mode coupling. Precis Eng 43:164–177. https://doi.org/10.1016/j.precisioneng.2015.07.006
9. Kim C-J, Oh J-S, Park C-H (2014) Modelling vibration transmission in the mechanical and control system of a precision machine. CIRP Ann 63(1):349–352. https://doi.org/10.1016/j.cirp.2014.03.133

10. Kam M, Saruhan H, İpekçi A (2019) Investigation the effect of 3d printer system vibrations on surface roughness of the printed products. Düzce Üniversitesi Bilim ve Teknoloji Dergisi 7:147–157
11. Pilch Z, Domin J, Szlapa A (2015) The impact of vibration of the 3d printer table on the quality of print. In: 2015 selected problems of electrical engineering and electronics (WZEE), IEEE, https://doi.org/10.1109/wzee.2015.7394045
12. Udroiu R, Braga I, Nedelcu A (2019) Evaluating the quality surface performance of additive manufacturing systems: Methodology and a material jetting case study. Materials 12(6):995. https://doi.org/10.3390/ma12060995
13. Çevik Ü, Kam M (2020) A review study on mechanical properties of obtained products by FDM method and metal/polymer composite filament production. J Nanomater 2020:1–9. https://doi.org/10.1155/2020/6187149
14. Johnson K, Blough J, Barnard A, Hartwig T, Brown B, Soine D, Collum T, Kinzel E, Bristow D, Landers R (2018) Frequency response inspection of additively manufactured parts for defect identification. In: Proceedings of the 29th annual international solid freeform fabrication symposium. University of Texas at Austin, https://doi.org/10.26153/TSW/17230
15. Allen A, Johnson K, Blough JR, Barnard A, Hartwig T, Brown B, Soine D, Cullom T, Bristow D, Landers R, Kinzel E (2020) Using BB-gun or acoustic excitation to find high frequency modes in additively manufactured parts. In: Sensors and instrumentation, aircraft/aerospace, energy harvesting & dynamic environments testing, vol. 7, Springer International Publishing, pp 77–84, https://doi.org/10.1007/978-3-030-47713-4_9
16. Petg specialty model material for makerbot. https://store.makerbot.com/petg
17. Townsend A, Senin N, Blunt L, Leach RK, Taylor JS (2016) Surface texture metrology for metal additive manufacturing: a review. Precis Eng 46:34–47. https://doi.org/10.1016/j.precisioneng.2016.06.001
18. Sanaei N, Fatemi A (2020) Analysis of the effect of surface roughness on fatigue performance of powder bed fusion additive manufactured metals. Theor Appl Fract Mech 108:102638. https://doi.org/10.1016/j.tafmec.2020.102638
19. Introducing makerbot method The first performance 3d printer. https://youtu.be/O4mRZE8S5yY
20. Inglasco sponge hockey puck. https://www.icewarehouse.com/Inglasco/descpage-SPGP.html